JOURNAL OF Applied Polymer SCIENCE

Kinetic Study on Free Radical Grafting of Polyethylene with Acrylic Acid by Reactive Extrusion

Guofang Zhang,[1] Min Zhang,[2] Yuxi Jia[1]

[1]School of Materials Science and Engineering, Shandong University, Jinan 250061, People's Republic of China

[2]School of Mechanical Engineering, Shandong University, Jinan 250061, People's Republic of China

Correspondence to: Y. Jia (E-mail: jia_yuxi@sdu.edu.cn)

ABSTRACT: In the reactive extrusion process for the free radical grafting of acid monomers onto polyethylene, monomer grafting and homopolymerization occur simultaneously and interact with each other. Using an incremental theory, mathematical models of conversions for monomer grafting and homopolymerization were separately constructed to predict the grafting degree, mass of homopolymer and grafting efficiency. Effects of the barrel temperature, initial monomer and initiator concentrations on grafting behaviors were investigated. The barrel temperature and initial monomer concentration were shown to be the main process parameters for controlling the grafting degree. The grafting degree and mass of homopolymer increased significantly with increasing barrel temperature and monomer concentration and increased marginally with increasing initiator concentration. No significant improvement in the grafting efficiency was observed. The predictions of the models are in good agreement with experimental data. © 2014 Wiley Periodicals, Inc. J. Appl. Polym. Sci. **2014**, *131*, 40990.

KEYWORDS: extrusion; grafting; kinetics; synthesis and processing; theory and modeling

Received 28 February 2014; accepted 6 May 2014

DOI: 10.1002/app.40990

INTRODUCTION

Twin-screw extrusion has been primarily used in the field of polymer modification to produce high-performance materials. The most widespread method of introducing functionality into polyolefins by reactive extrusion involves free radical grafting.[1–6] A major challenge in conducting grafting modifications is to devise process conditions to minimize or control side reactions while simultaneously maximize grafting yields.[7–11]

The competition between the grafting and homopolymerization often leads to poor grafting efficiency and makes the kinetic analysis of the overall process very complicated. However, the occurrence of homopolymerization can be controlled by varying processing parameters such as temperature, co-agent structure, feed concentration and residence time. Song and Baker developed the kinetic rate expressions for grafting and homopolymerization and explored conditions for maximizing grafting and minimizing homopolymerization for the grafting of dimethylaminoethyl methacrylate (DMAEMA) onto polyethylene (PE) in an intermeshing co-rotating twin-screw extruder.[12–14] Cha and White discussed the competition between the grafting and homopolymerization for the grafting of styrene onto polypropylene (PP). It was observed that the grafting degree increased with initial monomer and peroxide concentrations.[15] The grafting level of glycidyl methacrylate (GMA) onto linear low-density polyethylene (LLDPE) was also found to increase with initial GMA and peroxide concentrations. The unbound homopolymer was restrained with the use of a high-viscosity resin.[16] Shi et al. presented the grafting mechanism between LLDPE and acrylic monomers, and then carried out experiments to obtain the apparent chain propagation rate coefficients, reaction rates, reaction orders, and activation energies of grafting and homopolymerization.[17–20] Badel et al. synthesized graft copolymers with a poly(ethylene-*co*-1-octene) backbone and poly(methyl methacrylate) random polymer branches. With increasing initiator and monomer concentrations, the grafting degree increased and the grating efficiency decreased. Radical scavenger was used to limit the formation of PMMA homopolymer.[21]

Numerical simulations have been devoted to reactive extrusion processes for quantitatively analyzing the reaction trend and optimizing the processing conditions.[22–26] Such simulations have been performed by Motha and Seppala for the grafting of carboxylic acids and silanes to ethylene polymers,[27] Hojabr et al. for the grafting of GMA onto PE,[28] Fukuoka for the grafting between PE and vinylsilane,[29] Keum and White, Zhu et al., and Aguiar et al. for the grafting of maleic anhydride on PP,[30–32] and Zhao et al. for poly[ethylene-*co*-(vinyl alcohol)]-graft-poly(E-caprolactone).[33] With accurate numerical models, evolutions of key variables such as monomer conversion, grafting degree and fluid

viscosity can be quantitatively predicted. In addition, the effects of material composition, screw geometry and operating conditions on the progress of the reaction can be analyzed.

Few works have been paid to quantitatively understand the grafting reactions accompanied by homopolymerization in the twin-screw extruder. In fact, many monomers readily homopolymerize under the conditions employed in melt grafting. The intention of this article is to numerically analyze the kinetic behaviors in reactive extrusion processes for polymer grafting so as to maximize grafting yields while minimize homopolymerization. The grafting of acrylic acid (AA) onto LLDPE is chosen as the model system. Using an incremental theory, mathematical models of monomer conversions for grafting and homopolymerization are constructed separately to predict the grafting degree, mass of homopolymer and grafting efficiency. Using a semi-implicit iterative algorithm, the evolutions of the grafting and homopolymerization with time, barrel temperature, initial monomer and initiator concentrations are shown and numerically analyzed. Finally, the simulated results are compared with the experimental data to validate the rationality of the constructed models.

KINETIC MODELING OF AA GRAFTING ONTO LLDPE

Reaction Mechanisms

In the reactive extrusion process for the free radical grafting of acrylic monomers onto preirradiated polyethylene, monomer grafting and homopolymerization occur simultaneously. It is necessary to introduce some assumptions and approximations for simplification: (1) chain transfers to monomer are neglected for low rate constants;[18] (2) chain transfers to polymer are excluded because the relatively long graft chain was observed;[34] (3) termination reactions involving secondary polymeric radicals have minor importance for lower reactivity;[35] (4) coupling terminations involving polymeric radicals are ignored, for no crosslinking was present in the sample.[20] Therefore, the reaction mechanism can be considered as follows:[18]

$$\text{Peroxides formation} \quad \mathrm{P+O_2 \xrightarrow{irradiation} POOP+POOH} \tag{1}$$

$$\text{Decomposition of initiators} \quad \begin{aligned} &\mathrm{POOP \xrightarrow{k_{d1}} 2PO\cdot} \\ &\mathrm{POOH \xrightarrow{k_{d2}} PO\cdot + HO\cdot} \end{aligned} \tag{2}$$

$$\text{Initiation} \quad \begin{aligned} &\mathrm{PO\cdot + H\text{-}P \xrightarrow{k_{tr}} POH + P\cdot} \\ &\mathrm{P\cdot + M \xrightarrow{k_{i,g}} PM_1\cdot} \end{aligned} \tag{3}$$

$$\mathrm{HO\cdot + M \xrightarrow{k_{i,h}} HOM_1\cdot} \tag{4}$$

$$\text{Propagation} \quad \mathrm{PM_i\cdot + M \xrightarrow{k_{p,g}} PM_{i+1}\cdot} \tag{5}$$

$$\mathrm{HOM_i\cdot + M \xrightarrow{k_{p,h}} HOM_{i+1}\cdot} \tag{6}$$

$$\begin{aligned} &\mathrm{PM_i\cdot + PM_j\cdot \xrightarrow{k_t} PM_i + PM_j} \\ &\text{Termination } \mathrm{PM_i\cdot + HOM_j\cdot \xrightarrow{k_t} PM_i + HOM_j} \text{ or } \mathrm{PM_{i+j}OH} \\ &\mathrm{HOM_i\cdot + HOM_j\cdot \xrightarrow{k_t} HOM_i + HOM_j} \text{ or } \mathrm{HOM_{i+j}OH} \end{aligned} \tag{7}$$

where P and M represent the base polymer and monomer, respectively. POOP and POOH are two kinds of peroxide initiators generating on the polymer backbone by electron beam irradiation. PO· and HO· represent the primary free radicals, P·, PM·, and HOM· the secondary polymeric radicals, grafted polymeric radicals, and small free radicals, respectively. The rate constants for each elementary reaction are shown above the arrows. The mean rate constant for termination is used because of the complex termination mechanism.

The kinetic equations for the radical concentrations based on the above reaction steps are given by:[18]

$$\frac{dc_{\mathrm{PO}\cdot}}{dt} = 2f_1 k_{\mathrm{d1}} c_{\mathrm{POOP}} + f_2 k_{\mathrm{d2}} c_{\mathrm{POOH}} - k_{\mathrm{tr}}\, c_{\mathrm{PO}\cdot} c_{\mathrm{P}} \tag{8}$$

$$\frac{dc_{\mathrm{HO}\cdot}}{dt} = f_2 k_{\mathrm{d2}} c_{\mathrm{POOH}} - k_{\mathrm{i,h}}\, c_{\mathrm{HO}\cdot} c_{\mathrm{mono}} \tag{9}$$

$$\frac{dc_{\mathrm{P}\cdot}}{dt} = k_{\mathrm{tr}}\, c_{\mathrm{PO}\cdot} c_{\mathrm{P}} - k_{\mathrm{i,g}}\, c_{\mathrm{P}\cdot} c_{\mathrm{mono}} \tag{10}$$

$$\frac{dc_{\mathrm{PM}\cdot}}{dt} = k_{\mathrm{i,g}}\, c_{\mathrm{P}\cdot} c_{\mathrm{mono}} - k_{\mathrm{t}} c_{\mathrm{PM}\cdot}{}^2 - k_{\mathrm{t}} c_{\mathrm{PM}\cdot} c_{\mathrm{HOM}\cdot} \tag{11}$$

$$\frac{dc_{\mathrm{HOM}\cdot}}{dt} = k_{\mathrm{i,h}}\, c_{\mathrm{HO}\cdot} c_{\mathrm{mono}} - k_{\mathrm{t}} c_{\mathrm{HOM}\cdot}{}^2 - k_{\mathrm{t}} c_{\mathrm{PM}\cdot} c_{\mathrm{HOM}\cdot} \tag{12}$$

where f_1 and f_2 denote the initiator efficiencies of POOP and POOH, respectively. c_{POOP}, c_{POOH}, c_{mono} and c_{P} denote the concentrations of POOP and POOH, monomer and base polymer, respectively. $c_{\mathrm{PO}\cdot}$, $c_{\mathrm{HO}\cdot}$, $c_{\mathrm{P}\cdot}$, $c_{\mathrm{PM}\cdot}$ and $c_{\mathrm{HOM}\cdot}$ denote the concentrations of PO· and HO·, secondary polymeric radicals, grafted polymeric radicals and small free radicals, respectively.

AA is partially dissolved in molten PE and tends to form aggregates around the end sites of a polyethylene molecule.[36] Only monomers residing at the polyethylene/monomer interface or able to diffuse to the interface can react with grafted polymeric radicals, and only monomers that have captured the small free radicals can homopolymerize.[20] Therefore, the effective monomer concentration $c_{\mathrm{mono,e}}$ that participates in the overall reaction has to be defined, and its formula is given by:

$$c_{\mathrm{mono,e}} = K c_{\mathrm{mono,0}} \tag{13}$$

where K and $c_{\mathrm{mono,0}}$ denote the effective coefficient and initial monomer concentration, respectively. Shi et al. determined the effective monomer concentration by summing the monomer concentration participating in the grafting and that in the homopolymerization.[20] Here K was calculated by fitting the data of the consumed AA in different experiment runs.

For the high viscosity as well as the low monomer concentration, the two-molecular termination is difficult. ESR results showed that the concentration of propagation free radicals only

slightly changed. According to the assumption that all radicals are at a steady-state, the following expressions can be obtained:

$$c_{PM\cdot}=\frac{2f_1k_{d1}c_{POOP}+f_2k_{d2}c_{POOH}}{k_t(c_{PM\cdot}+c_{HOM\cdot})} \quad (14)$$

$$c_{HOM\cdot}=\frac{f_2k_{d2}c_{POOH}}{k_t(c_{PM\cdot}+c_{HOM\cdot})} \quad (15)$$

$$c_{PM\cdot}+c_{HOM\cdot}=\left[\frac{2(f_1k_{d1}c_{POOP}+f_2k_{d2}c_{POOH})}{k_t}\right]^{1/2} \quad (16)$$

Construction of Mathematical Models

Models for Overall Monomer Conversion. The overall rate taking both the grafting and homopolymerization into account can be written as:

$$-\frac{dc_{mono}}{dt}=k_pc_{mono}(c_{PM\cdot}+c_{HOM\cdot})=k_p\left[\frac{2(f_1k_{d1}c_{POOP}+f_2k_{d2}c_{POOH})}{k_t}\right]^{1/2}c_{mono} \quad (17)$$

The magnitude of $k_{p,g}$ and $k_{p,h}$ is in the same order.[18] The mean rate constant for propagation k_p is introduced for simplification.

Taking the effective monomer concentration as the research object, a local monomer conversion x can be deduced:

$$\frac{dx}{dt}=k_p\left[\frac{2(f_1k_{d1}c_{POOP}+f_2k_{d2}c_{POOH})}{k_t}\right]^{1/2}(1-x) \quad (18)$$

Combining with eq. (13), the global monomer conversion X corresponding to the feed monomer concentration can be derived:

$$X=Kx \quad (19)$$

Substituting eq. (19) into eq. (18) then:

$$\frac{dX}{dt}=k_p\left[\frac{2(f_1k_{d1}c_{POOP}+f_2k_{d2}c_{POOH})}{k_t}\right]^{1/2}(K-X) \quad (20)$$

Arrhenius equation gives the dependence of rate constants on temperature. For an isothermal process, if the initiator concentration is a known constant, the overall monomer conversion can be calculated directly with eq. (20). But in reactive extrusion processes, the temperature and initiator concentration are variable, therefore the overall monomer conversion can not be calculated directly via eq. (20).

An incremental theory is introduced to solve the above mentioned problems.[37] Unfold the fluid flow space along the axial direction of the screw channel as a two-dimensional axisymmetrical laminar flow model and then discretize it.[24] Assuming that $X(I,J)$ denotes the overall monomer conversion on the Jth space point in the Ith time step, $X(I-1,J)$ the overall monomer conversion on the Jth space point in the $(I-1)$th time step, and $\Delta X(I,J)$ the increment of overall monomer conversion on the Jth space point in the Ith time step, the following equation can be obtained:

$$\left.\frac{\partial X}{\partial t}\right|_{I,J}=\frac{\Delta X(I,J)}{\Delta t}+O(\Delta t)=\frac{X(I,J)-X(I-1,J)}{\Delta t}+O(\Delta t) \quad (21)$$

where Δt denotes the time step, and $O(\Delta t)$ the truncation error for the finite-difference equation.

Submitting eq. (20) into eq. (21) leads to the numerical computation expression of the increment of the overall monomer conversion:

$$\Delta X(I,J)=\frac{k_p(I,J)\left\{\frac{2[f_1k_{d1}(I,J)c_{POOP}(I,J)+f_2k_{d2}(I,J)c_{POOH}(I,J)]}{k_t(I,J)}\right\}^{1/2}\Delta t(I,J)[K-X(I-1,J)]}{1+k_p(I,J)\left\{\frac{2[f_1k_{d1}(I,J)c_{POOP}(I,J)+f_2k_{d2}(I,J)c_{POOH}(I,J)]}{k_t(I,J)}\right\}^{1/2}\Delta t(I,J)} \quad (22)$$

where the temperature $T(I,J)$ is contained in the rate constants according to the Arrhenius formulation. If the time step $\Delta t(I,J)$ is adequately small, $T(I,J)$, $c_{POOP}(I,J)$ and $c_{POOH}(I,J)$ on the Jth space point can be approximately considered as constants in the Ith time step.

Models for Conversions of Grafting and Homopolymerization. Define R_g and R_h as the reaction rates for the grafting and homopolymerization, respectively. The conversions for monomer grafting and homopolymerization in any time step can be separately calculated via eq. (23) and eq. (24):

$$X_g(I,J)=X_g(I-1,J)+\frac{R_g}{R_g+R_h}\Delta X(I,J) \quad (23)$$

$$X_h(I,J)=X_h(I-1,J)+\frac{R_h}{R_g+R_h}\Delta X(I,J) \quad (24)$$

where the ratio of R_g to R_h is obtained from eq. (14) and eq. (15):

$$\frac{R_g}{R_h}=\frac{k_{p,g}c_{PM\cdot}}{k_{p,h}c_{HOM\cdot}}=\frac{k_{p,g}(2f_1k_{d1}c_{POOP}+f_2k_{d2}c_{POOH})}{k_{p,h}f_2k_{d2}c_{POOH}} \quad (25)$$

Models for Grafting Degree, Mass of Homopolymer and Grafting Efficiency. According to the definitions of grafting degree G_d, mass of homopolymer M_h and grafting efficiency G_e, we can obtain their numerical computation expressions:

$$G_d(I,J)=\frac{\text{mass of monomer grafted}}{\text{mass of initial polymer}}=c_{mono,0}\,X_g(I,J)M_{mono} \quad (26)$$

$$M_h(I,J)=\frac{\text{mass of monomer homopolymerized}}{\text{mass of initial polymer}}=c_{mono,0}\,X_h(I,J)M_{mono} \quad (27)$$

$$G_e(I,J)=\frac{\text{mass of monomer grafted}}{\text{total mass of monomer reacted}}=\frac{X_g(I,J)}{X_g(I,J)+X_h(I,J)} \quad (28)$$

where M_{mono} denotes the molecular weight of monomer. Take

Table I. Parameters of the Twin Screw Extruder for the Grafting Reaction[20]

Parameters	Numerical values
Nominal diameter of screws	24 mm
Centerline distance of screws	18.75 mm
Slenderness ratio of screws	40
Number of thread starts	2
Lead of screws	24 mm

notice that the unit of the initial monomer concentration is mol g^{-1} (mols of monomer per gram of polymer).

CONSTRUCTION OF CHEMORHEOLOGICAL MODEL

In order to describe the rheological property of the incompressible non-Newtonian fluids, the power-law constitutive equation is adopted[3,38]

$$\eta(I,J)=\frac{a}{[1+b\dot{\gamma}(I,J)]^c} \tag{29}$$

where η denotes the apparent viscosity, $\dot{\gamma}$ the shear rate. a, b and c are three parameters. When $\dot{\gamma}=0$, $a=\eta_0$.

The weight ratio of grafted monomer to polymer is very low,[20] so the zero shear viscosity η_0 depends mainly on temperature and the weight-average molecular weight $\overline{M}_w$ of PE[29]

$$\eta_0(I,J)=\begin{cases} K_1 e^{\frac{E_\eta}{RT(I,J)}}\overline{M}_w(I,J) & \overline{M}_w(I,J)\le M_c \\ K_2 e^{\frac{E_\eta}{RT(I,J)}}\overline{M}_w(I,J)^{3.4} & \overline{M}_w(I,J)> M_c \end{cases} \tag{30}$$

where K_1 and K_2 denote the material constants, E_η the activation energy for fluid flow, M_c the critical molecular weight for entanglement effects in viscosity.

SETUP OF NUMERICAL SIMULATION

Conditions for Experiment and Simulation

To validate the rationality of the constructed models, the simulated results were compared with Shi et al.'s experimental data.[20] The grafting of LLDPE with AA was carried out in a modular co-rotating twin screw extruder whose parameters are shown in Table I.[20] The input data related to material properties are shown in Table II.[17–20,39]

Considering the melt time of LLDPE, the grafting reaction starts at the position $L/D=14$.[20] So the grafting reaction occurs in the zone between 0.34 m and 0.96 m along the axial length of the extruder. The fluid flows forward in the extruder by means of both the drag effect of screws and the pressure effect. In the simulation, the space of fluid flow was equivalently considered as a long axisymmetrical space, in which the effect of the axial motion of the solid wall on fluid flow was equivalent to the integrated effect of the screws and barrels on fluid flow. According to the construction method of the reactor model in our

Table II. Material Properties for the Grafting Reaction[17–20,39]

Parameters	Numerical values
Density of polyethylene	920 $kg.m^{-3}$
Density of monomer	1051 $kg.m^{-3}$
Molecular weight of polyethylene	1.17×10^5 $g.mol^{-1}$
Molecular weight of monomer	72 $g.mol^{-1}$
Initiator efficiency	1.0
Frequency factor for dialkyl peroxide decomposition	1.091×10^{15} s^{-1}
Frequency factor for hydroperoxide decomposition	1.003×10^{13} s^{-1}
Activation energy for dialkyl peroxide decomposition	1.475×10^5 $J.mol^{-1}$
Activation energy for hydroperoxide decomposition	1.297×10^5 $J.mol^{-1}$
Frequency factor for grafting propagation	3.171×10^{11} $g.mol^{-1}.s^{-1}$
Activation energy for grafting propagation	4.256×10^4 $J.mol^{-1}$
Frequency factor for homopolymerization propagation	4.552×10^{12} $g.mol^{-1}.s^{-1}$
Activation energy for homopolymerization propagation	$5.120\times10^4 J.mol^{-1}$
Mean frequency factor for propagation	1.518×10^{12} $g.mol^{-1}.s^{-1}$
Mean activation energy for propagation	4.769×10^4 $J.mol^{-1}$
Mean frequency factor for termination	3.178×10^{18} $g.mol^{-1}.s^{-1}$
Mean activation energy for termination	6.913×10^4 $J.mol^{-1}$
The parameter b in viscosity equation	0.2649 s
The parameter c in viscosity equation	0.7899
Critical molecular weight for entanglement effects	40,000 $g.mol^{-1}$
Activation energy for fluid flow	2.775×10^4 $J.mol^{-1}$

previous study,[24] the equivalent length and radius of the model could be calculated.

Monomer was premixed with LLDPE and fed at the entrance of the extruder.[20] In the simulation, it is assumed that the monomer and polymer were well mixed in every element of the reactor model during the whole extrusion process. The inlet velocity of the reactor model is calculated by the throughput, and the velocity of the wall is determined according to the screw speed as well as the degree of the wall slip.

The study of reaction mechanism [eq. (17)] indicates that the grafting behaviors mainly depend on the temperature, residence time, monomer concentration and initiator concentration. In order to compare with Shi et al.'s experimental data,[20] the barrel temperature, initial monomer and initiator concentrations were chosen as main process conditions in the simulation.

Steps for Numerical Simulation

A semi-implicit iterative algorithm is proposed to deal with the complicated relationships among the variables such as pressure, flow velocity, temperature, reaction rate, average molecular weight, and fluid viscosity. The specific steps are shown as follows:

1. Initialize fields of pressure, velocity and viscosity, variables such as initial concentrations of polymer, monomer and initiator, and then set boundary conditions.
2. Iteratively solve the continuity equation and momentum conservation equation to get the convergent fields of pressure, velocity and shear rate and temperature. Detailed descriptions of the numerical calculation have been reported in Ref. 40.
3. Solve the kinetic equations [eq. (22–24)] to obtain the conversions for monomer grafting and homoploymerization, grafting degree, mass of homopolymer and grafting efficiency.
4. Solve the chemorheological equations [eqs. (29) and (30)] to obtain the zero shear viscosity and apparent viscosity of the fluids.
5. Judge the results whether they satisfy the convergence conditions or not. If they do, end the calculation and output the results, whereas, readjust the viscosity value in the momentum conversation equation and recompute from the second step.

The detailed flow chart of the numerical simulation is shown in Fig. 1.

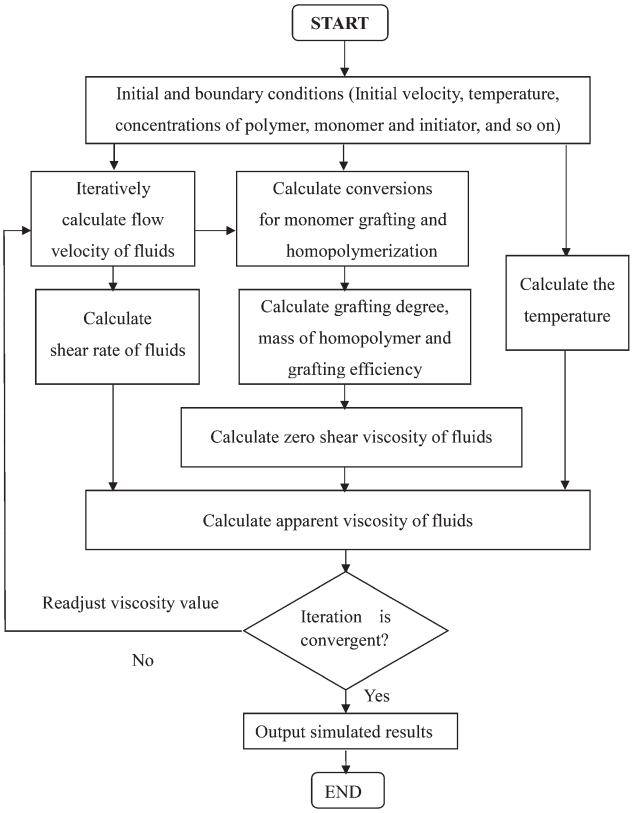

Figure 1. Flow chart of numerical simulation.

RESULTS AND DISCUSSION

Evolutions of Key Variables

When the irradiation dose is 15 kGy, the barrel temperature of the extruder is 190 °C and the initial monomer concentration is 7.5×10^{-4}mol.g^{-1}, the evolutions of the grafting degree and mass of homopolymer along the axial direction of the extruder are shown in Fig. 2. It can be seen that both the grafting degree and mass of homopolymer increase along the axial direction of the extruder. The reason is as follows: the monomer conversions for grafting and homopolymerization are increasing functions of reaction time [eq. (22)].

Influences of Processing Parameters

Influence of Barrel Temperature. The grafting degree and mass of homopolymer are seen to increase significantly with increasing temperature (Figs. 3 and 4). Arrhenius equation explains the variation of rate constants with temperature. Monomer conversions for grafting and homopolymerization are increasing functions of temperature [eqs. (22–24)].

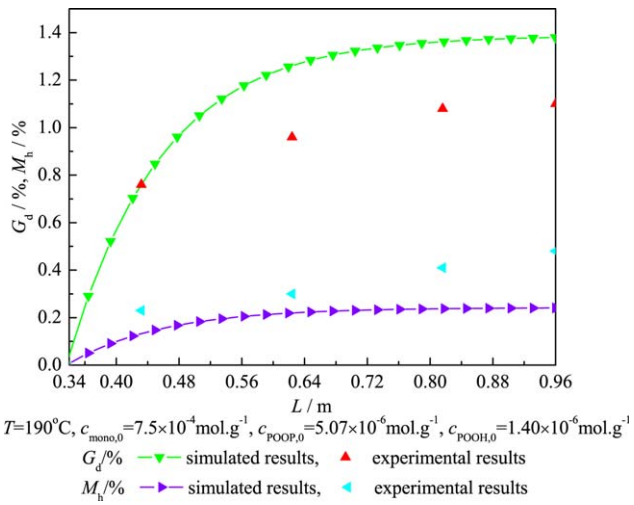

Figure 2. Evolution of grafting degree and mass of homopolymer along the axial direction of the extruder. [Color figure can be viewed in the online issue, which is available at wileyonlinelibrary.com.]

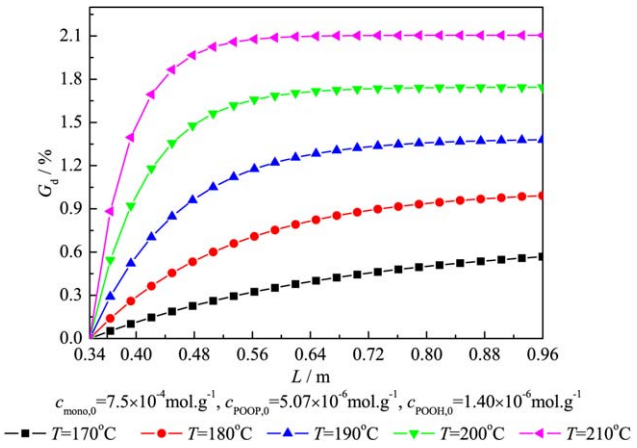

Figure 3. Influence of barrel temperature on grafting degree. [Color figure can be viewed in the online issue, which is available at wileyonlinelibrary.com.]

The grafting efficiency shows a minor change with increasing temperature (Fig. 5). The ceiling temperature at which the rates of depropagation and propagation are equal has an important effect on the grafting behavior. If the melt grafting runs close to this temperature, the grafting efficiency can increase with increasing temperature due to the onset of the depropagation reaction.[14] However, in the process of LLDPE grafting with AA, the depropagation reaction hardly occurs because the ceiling temperature of AA is close to 400°C,[35] far higher than the set temperature. Therefore, the simultaneous increase in both grafting degree and mass of homopolymer causes the nearly invariable grafting efficiency.

Influence of Initial Monomer Concentration. The higher the initial monomer concentration, the higher the grafting degree and mass of homopolymer are (Figs. 6 and 7). Higher monomer concentration gradient leads to more amount of monomer aggregating near the end sites of the polymer chains, enhancing the collision probability between the radicals and monomer. From mathematical point of view, both the grafting degree and mass of homopolymer are directly proportional to initial monomer concentration [eqs. ((26) and (27))].

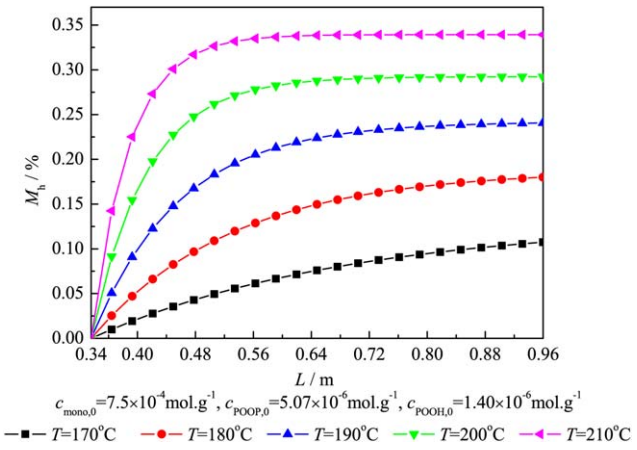

Figure 4. Influence of barrel temperature on mass of homopolymer. [Color figure can be viewed in the online issue, which is available at wileyonlinelibrary.com.]

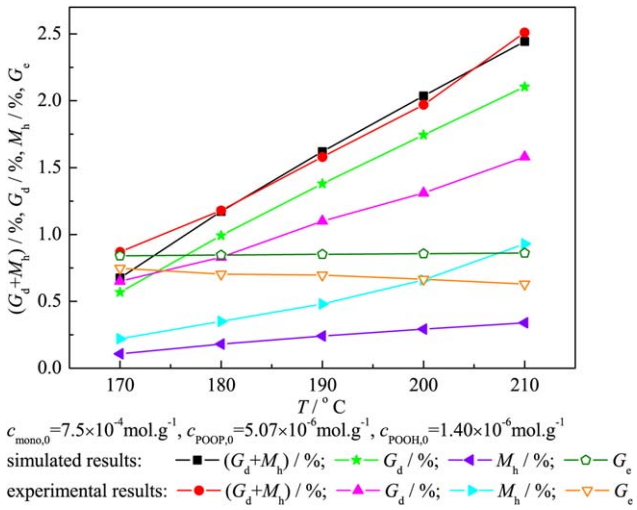

Figure 5. Comparison between simulated and experimental results under different barrel temperatures. [Color figure can be viewed in the online issue, which is available at wileyonlinelibrary.com.]

With increasing initial monomer concentration, it can be seen from Fig. 8 that both the grafting degree and mass of homopolymer increase significantly while the grafting efficiency decreases only marginally. The reaction rates for initiation mainly control the grafting behavior because the propagation rate constants of grafting and homopolymerization are almost identical.[18] There are two steps for grafting initiation: the first is the hydrogen abstraction from the polymer backbone to form the secondary polymeric radical, the second is the attack of monomer. If the first step mainly controls the grafting initiation, such as in the grafting of LLDPE with DMAEMA, the grafting degree is not greatly affected by increasing the monomer concentration, but the rate of the homopolymerization initiation increases

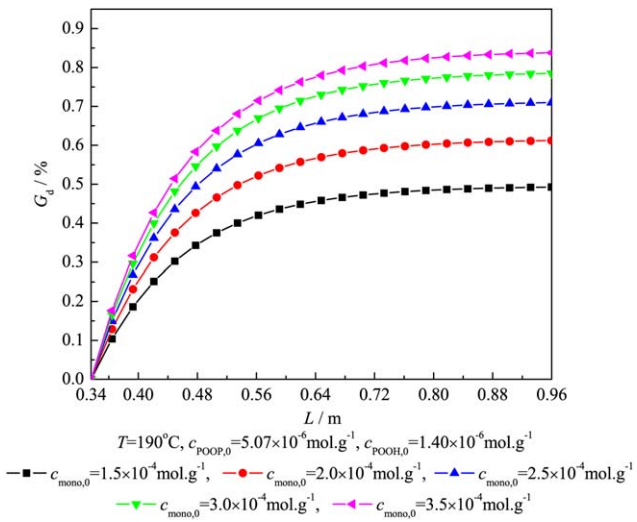

Figure 6. Influence of initial monomer concentration on grafting degree. [Color figure can be viewed in the online issue, which is available at wileyonlinelibrary.com.]

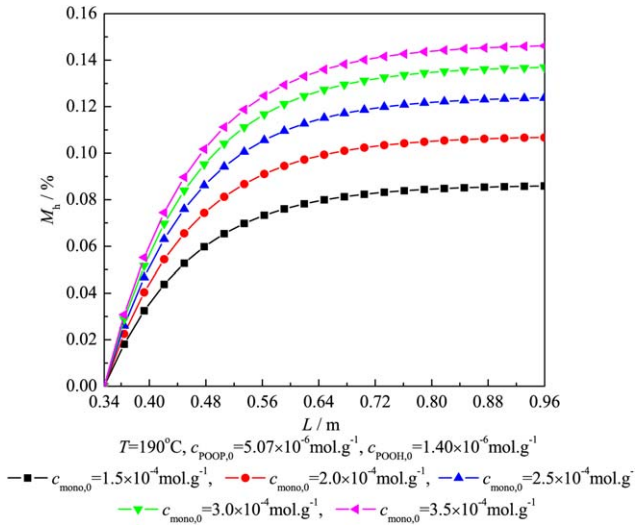

Figure 7. Influence of initial monomer concentration on mass of homopolymer. [Color figure can be viewed in the online issue, which is available at wileyonlinelibrary.com.]

obviously. The combination of these two effects leads to a dramatic decrease in the grafting efficiency.[14] However, in the grafting of LLDPE with AA, the second step dominates the grafting initiation.[20] More monomers can participate in the reaction with increasing initial monomer concentration, so both the grafting degree and mass of homopolymer increase obviously while the grafting efficiency stays relatively unchanged.

Influence of Initial Initiator Concentration. Increases in the grafting degree and mass of homopolymer are observed with increasing initial initiator concentration (Figs. 9 and 10). When the initiator concentration is higher, more monomers can participate in the reaction due to the increasing primary radicals. From mathematical point of view, both the grafting degree and

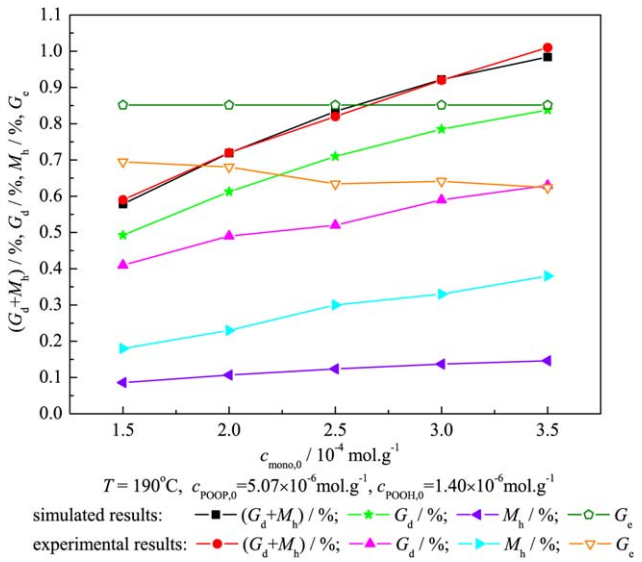

Figure 8. Comparison between simulated and experimental results under different initial monomer concentrations. [Color figure can be viewed in the online issue, which is available at wileyonlinelibrary.com.]

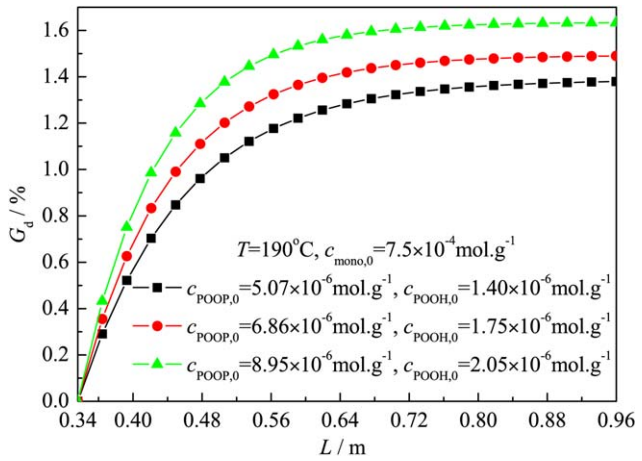

Figure 9. Influence of initial initiator concentration on grafting degree. [Color figure can be viewed in the online issue, which is available at wileyonlinelibrary.com.]

mass of homopolymer are increasing functions of the initiator concentration [eqs. (22–24)].

The increasing range is limited because the monomer is partially miscible with the melt polymer. Therefore, both grafting degree and mass of homopolymer increase slightly and this synchronous increase trend results in little changes of the grafting efficiency (Fig. 11).

Comparison with Experimental Results

Comparisons between the simulated and experimental results under varied barrel temperatures, initial monomer concentrations and initial initiator concentrations are shown in Figs. 5, 8, and 11, respectively. It can be seen that:

1. The trend of the simulated results meets well with that of the experimental results.
2. The mass of monomer participating in the overall reaction predicted from the simulation is in good agreement with that obtained from the experiment.

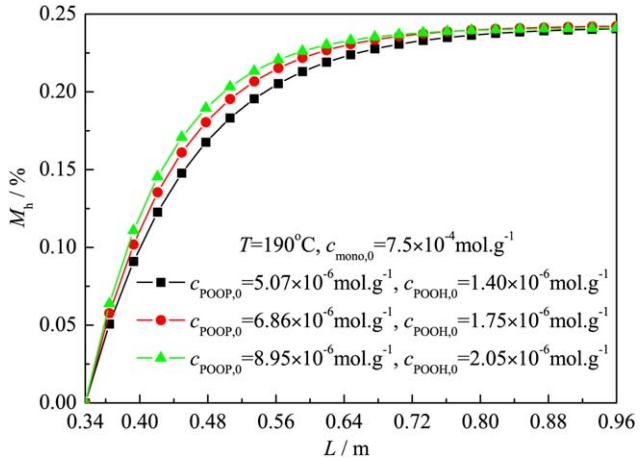

Figure 10. Influence of initial initiator concentration on mass of homopolymer. [Color figure can be viewed in the online issue, which is available at wileyonlinelibrary.com.]

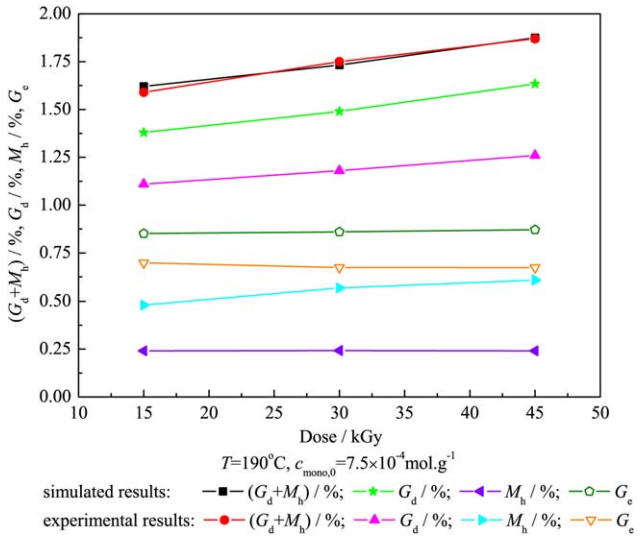

Figure 11. Comparison between simulated and experimental results under different initial initiator concentrations. [Color figure can be viewed in the online issue, which is available at wileyonlinelibrary.com.]

3. The predicted grafting degree and grafting efficiency are higher while the predicted mass of homopolymer is smaller than the experimental result.

The reason is as follows: AA is premixed with PE and partially dissolved in molten PE. Therefore, the grafting progresses in two stages: the initial stage and the diffusion-controlled stage. AA tends to form aggregates around the end sites of PE chains, so the initial stage can be described by the conventional kinetic equations. When the disappearance rate of monomer exceeds the diffusion rate of monomer, the grafting becomes diffusion-controlled. The collision probability between the polymeric free radicals and monomer decreases while that between the small free radicals and monomer almost keeps constant, which resulting in the decrease of $k_{p,g}$ and small change of $k_{p,h}$. In the simulation, the assumption that all radicals are at a steady-state is adopted, and $k_{p,g}$ and $k_{p,h}$ are almost identical during the whole process. According to eq. (25), R_g/R_h calculated via simulation is higher than that obtained from experiment.

4. The differences between the simulated and experimental results increase with increasing barrel temperature and initial monomer concentration while those show little changes with the variation of initial initiator concentration.

The exact transition time from the initial stage to the diffusion-controlled stage is influenced by temperature, the initial monomer concentration, the rate of grafting and the diffusion rate of monomer and can not be explicitly predicted,[19] which make the reasons of the above differences are not quite clear so far. The development of models involving diffusion effect in an extruder becomes the urgent matter.

CONCLUSION

1. Using an incremental theory, mathematical models of conversions for monomer grafting and homopolymerization were separately constructed to predict the time-evolutions of grafting degree, mass of homopolymer and grafting efficiency.
2. The simulated results show that the increases of the barrel temperature, monomer concentration, and initiator concentration positively influence the grafting degree and mass of homopolymer but have no noticeable effect on the grafting efficiency, and that the barrel temperature and the monomer concentration largely control the reaction while the initiator concentration only has a small effect.
3. Comparison with experimental data indicates that the models can predict the kinetic behavior well, which validates the rationality of the constructed models. Coupling with an optimization methodology, the models can be used to optimize process conditions to minimize homopolymerization while maximize grafting yield.

ACKNOWLEDGMENTS

This work was supported by the National Natural Science Foundation of China (51103080), the Natural Science Foundation of Shandong Province (JQ201016) and the China Postdoctoral Science Foundation (20110491563).

REFERENCES

1. Moad, G. *Prog. Polym. Sci.* **1999**, *24*, 81.
2. Machado, A. V.; Covas, J. A.; VanDuin, M. *Adv. Polym. Technol.* **2004**, *23*, 196.
3. Cassagnau, P.; Bounor-Legare, V.; Fenouillot, F. *Int. Polym. Proc.* **2007**, *22*, 218.
4. Passaglia, E.; Coiai, S.; Augier, S. *Prog. Polym. Sci.* **2009**, *34*, 911.
5. Sadik, T.; Massardier, V.; Becquart, F.; Taha, M. *J. Appl. Polym. Sci.* **2013**, *129*, 2177.
6. Passaglia, E.; Coiai, S.; Cicogna, F.; Ciardelli, F. *Polym. Int.* **2014**, *63*, 12.
7. Badel, T.; Beyou, E.; Bounor-Legare, V.; Chaumont, P.; Flat, J. J.; Michel, A. *J. Polym. Sci. Part A: Polym. Chem.* **2007**, *45*, 5215.
8. Sheshkali, H. R. Z.; Assempour, H.; Nazockdast, H. *J. Appl. Polym. Sci.* **2007**, *105*, 1869.
9. Burton, E.; Woodhead, M.; Coates, P.; Gough, T. *J. Appl. Polym. Sci.* **2010**, *117*, 2707.
10. Cicogna, F.; Coiai, S.; Passaglia, E.; Tucci, I.; Ricci, L.; Ciardelli, F.; Batistini, A. *J. Polym. Sci. Part A: Polym. Chem.* **2011**, *49*, 781.
11. Sirisinha, K. and Boonkongkaew, M. *J. Polym. Res.* **2013**, *20*, 120.
12. Song, Z. and Baker, W. E. *J. Appl. Polym. Sci.* **1990**, *41*, 1299.
13. Wong Shing, J. B.; Baker, W. E.; Russell, K. E. *J. Polym. Sci. Part A: Polym. Chem.* **1995**, *33*, 633.
14. Oliphant, K. E.; Russell, K. E; Baker, W. E. *Polymer* **1995**, *36*, 1597.
15. Cha, J. and White, J. L. *Polym. Eng. Sci.* **2001**, *41*, 1238.

16. Pesneau, I.; Champagne, M. F.; Huneault, M. A. *J. Appl. Polym. Sci.* **2004**, *91*, 3180.
17. Shi, Q.; Zhu, L.; Cai, C.; Yin, J.; Costa, G. *Polymer* **2006**, *47*, 1979.
18. Shi Q.; Cai C.; Zhu L.; Yin J. *Macromol. Chem. Phys.* **2007**, *208*, 1803.
19. Shi, Q.; Zhu, L.; Cai, C.; Yin, J. *Chinese. J. Polym. Sci. (Eng Ed)* **2005**, *23*, 603.
20. Shi, Q.; Zhu, L.; Cai, C.; Yin, J.; Costa, G. *J. Appl. Polym. Sci.* **2006**, *101*, 4301.
21. Badel, T.; Beyou, E.; Bounor-Legaré, V.; Chaumont, P.; Cassagnau, P.; Flat, J. J.; Michel, A. *Macromol. Mater. Eng.* **2012**, *297*, 702.
22. Zhu, L.; Narh, K. A.; Hyun, K. S. *Adv. Polym. Technol.* **2005**, *24*, 183.
23. Vergnes, B. and Berzin, F. C. R. *Chim.* **2006**, *9*, 1409.
24. Jia, Y.; Zhang, G.; Wu, L.; Sun, S.; Zhao, G.; An, L. *Polym. Eng. Sci.* **2007**, *47*, 667.
25. Banu, I.; Puaux, J. P.; Bozga, G.; Nagy, I. *Macromol. Symp.* **2010**, *289*, 108.
26. Ortiz-Rodriguez, E. and Tzoganakis, C. *Int. Polym. Proc.* **2012**, *27*, 442.
27. Motha, K. and Seppala, J. *Polym. Eng. Sci.* **1989**, *29*, 1579.
28. Hojabr, S.; Baker, W. E.; Russell, K. E.; McLellan, P. J.; Huneault, M. A. *Int. Polym. Proc.* **1998**, *13*, 118.
29. Fukuoka, T. *Polym. Eng. Sci.* **2000**, *40*, 2524.
30. Keum, J. and White, J. L. *J. Vinyl Addit. Technol.* **2005**, *11*, 143.
31. Zhu Y.; An L.; Jiang W. *Macromolecules* **2003**, *36*, 3714.
32. Aguiar, L. G.; Pessôa-Filho, P. A.; Giudici, R. *Macromol. Theory Simul.* **2011**, *20*, 837.
33. Zhao, Y.; Becquart, F.; Chalamet, Y.; Chen, J. D.; Taha, M. *Macromol. Mater. Eng.* **2009**, *294*, 651.
34. Huang, H.; Yao, Z.; Yang, J.; Wang, Y.; Shi, D.; Yin, J. *J. Appl. Polym. Sci.* **2001**, *80*, 2538.
35. Russell, K. E. *Prog. Polym. Sci.* **2002**, *27*, 1007.
36. Nath, S. K. and De Pablo, J. J. *J. Phys. Chem. B* **1999**, *103*, 3539.
37. Jia, Y.; Sun, S.; Liu, L.; Xue, S.; Zhao, G. *Polymer* **2003**, *44*, 319.
38. Vergnes, B.; Della Valle, G.; Delamare, L. *Polym. Eng. Sci.* **1998**, *38*, 1781.
39. Wu, Q.; Wu, J. Polymer Rheology; Higher Education Press: Beijing, **2002**, p 36.
40. Wu, L.; Jia, Y.; Sun, S.; Zhang, G.; Zhao, G.; An, L. *J. Appl. Polym. Sci.* **2007**, *103*, 2331.